JOURNAL OF AIRCRAFT
Vol. 35, No. 5, September–October 1998

Transition Closure Model for Predicting Transition Onset

E. S. Warren* and H. A. Hassan†
North Carolina State University, Raleigh, North Carolina 27695-7910

A unified approach that makes it possible to determine the extent and onset of transition in one calculation is presented. It treats the nonturbulent fluctuations in a manner similar to that used in describing turbulence. As a result, the complete flowfield can be calculated using existing computational fluid dynamics codes and without the use of stability codes. The method is validated by comparing the results for flat plates, airfoils, and infinite swept wings with available experiments. In general, good agreement is indicated.

Introduction

TRADITIONALLY, the transition problem has been treated as a combination of two problems. The first deals with the extent of the transition region given the onset, whereas the second deals with the transition onset. One of the methods employed in calculating the extent is to set the effective viscosity, μ, in a boundary-layer (BL) code or Navier–Stokes (NS) solver as

$$\mu = \mu_l + \Gamma\mu_t \tag{1}$$

where subscripts l and t designate laminar and turbulent flows, respectively, and Γ is the intermittency or the fraction of time the flow is turbulent at a given location. The most widely used expression for Γ is that of Dhawan and Narasimha.[1]

There are many ways being used to specify transition onset: arbitrary selection, experimental correlations, or the use of stability theory. Methods based on stability theory employ the e^n method or a method based on the parabolized stability equations (PSE). Methods based on stability theory have shown a great deal of promise when streamwise or Tollmien–Schlichting (T–S) waves are the dominant cause of transition. The same cannot be said when transition is a result of crossflow (CF) instabilities because such instabilities are dominated by nonlinear effects and surface roughness. An excellent recent review of these methods and their limitations is given by Haynes et al.[2]

In situations where transition onset is specified from results of an experiment, Eq. (1) does not perform well. One of the reasons for this behavior is because the preceding formula does not account for the nonturbulent fluctuations that eventually lead to transition. This led Young et al.[3] and Warren et al.[4] to employ an expression for μ given by

$$\mu = \mu_l + [(1 - \Gamma)\mu_{lf} + \Gamma\mu_t] \tag{2}$$

where μ_{lf} is the contribution of the nonturbulent fluctuations. The expression for μ_{lf} was correlated by using results from linear stability theory for both low- and high-speed flows. Much better agreement with experiment was indicated when Eq. (2) was employed.

The inability of stability theory to cope with crossflow instabilities led Warren and Hassan[5,6] to develop a new approach for determining transition onset. This approach is centered around the determination of μ_{lf}. When μ_{lf} is known, then the onset of transition, which may correspond to minimum skin friction, minimum heat flux, or some other criterion specified by the user, can be determined as part of the solution. Such an approach then removes the need for stability codes to predetermine transition onset. Moreover, it addresses transition onset and extent as one, not two, separate problems.

In both transition and turbulence, each flow quantity is set as a sum of a mean and fluctuating quantity. The exact equations governing fluctuations are the same. In transition, attention is focused on individual modes and frequencies with the growth rates of such modes playing a crucial role in determining transition onset. In turbulence, equations governing fluctuations are used to derive equations for the mean energy of the fluctuations and its dissipation rate. As a result, individual modes do not play any direct role in turbulence calculations. The resulting equations governing turbulence are not closed, thus necessitating assumptions on a constitutive stress–strain relation.

The approach presented here takes advantage of similarities between laminar and turbulent fluctuations; i.e., the exact equations governing energy and its dissipation rate are identical. Moreover, it is possible to model these exact equations[7] without invoking the nature of fluctuations. To close the model equations, it is necessary to provide constitutive stress–strain relations. To facilitate implementation in existing computational fluid dynamics (CFD) codes, an eddy viscosity model will be employed.

In the present work, the constitutive stress–strain relations for the nonturbulent fluctuations are derived from observed or computed characteristics of T–S and CF disturbances. Because mechanisms responsible for transition are different for the two types of instabilities, corresponding stress–strain relations are different. In both cases, however, μ_{lf} is set as

$$\mu_{lf} = C_\mu \rho k \tau \tag{3}$$

where k is the fluctuation kinetic energy per unit mass, ρ is the density, and τ is a time-scale characteristic of the type of instabilities being considered. Although the present approach makes no direct use of stability codes, expressions for τ were modeled using results obtained from stability theory or from experimental observations.

It is to be noted that this is not the first attempt at using equations similar to the turbulence equations to predict transition onset. Typical of these attempts is the work of Wilcox.[8–10] An earlier attempt attempted to take advantage of the results of linear stability theory.[9] In the latest effort, the approach used in Ref. 9 was abandoned in favor of an approach in which the model constants in the k-ω model were replaced by functions of the turbulence Reynolds number.[10] The func-

Received March 19, 1998; revision received May 18, 1998; accepted for publication June 22, 1998.

*Research Assistant, Mechanical and Aerospace Engineering; currently Chief, Engineering and Testing, Kranefuss Haas Racing, Inc., Mooresville, NC 28115.

†Professor, Mechanical and Aerospace Engineering. Associate Fellow AIAA.

tions were selected in such a way so as to reduce to the original model constants at high turbulence Reynolds number and, to reproduce transition onset for an incompressible flow over a flat plate. As formulated, the model is insensitive to the modes of transition[11] and, thus, will not yield good results outside the range for which it was formulated.[12] This may be contrasted with the present model in which separate equations are used to model the nonturbulent fluctuations and where the stress–strain relations that govern those fluctuations are not only sensitive to the various modes of transition but are dictated by them.

It should be emphasized that the approach presented here applies to situations where one mechanism of instability is dominant. Linear stability theory does not provide any guidance when two mechanisms are operative. Therefore, linear superimposition should not be attempted for such situations. In addition, the approach requires for its implementation two measurements: tunnel intensity and surface roughness.

Problem Formulation

The basis for the present approach is the exact equations governing k and ζ, the entrophy or the variance of vorticity. The k-ζ turbulence model employed in this work is that of Robinson and Hassan.[13] The equations that model k and ζ can be rewritten for low-speed flows as[13]

$$\frac{Dk}{Dt} = -\overline{u_i' u_j'}\,\frac{\partial U_i}{\partial x_j} - \frac{k}{\tau_k} + \frac{\partial}{\partial x_j}\left[\left(\frac{\nu}{3} + \frac{\nu_t}{\sigma_k}\right)\frac{\partial k}{\partial x_j}\right] \tag{4}$$

$$\begin{aligned}\frac{D\zeta}{Dt} &= \frac{\partial \Omega_i}{\partial x_j}\left\{\frac{\nu_t}{\sigma_r}\left[\frac{\partial \Omega_i}{\partial x_j} + \frac{\partial \Omega_j}{\partial x_i}\right] - \varepsilon_{mij}\left[\frac{\partial(\overline{u_m' u_l'})}{\partial x_l} - \frac{\partial k}{\partial x_m}\right]\right\}\\
&\quad + \frac{\partial}{\partial x_j}\left[\left(\nu + \frac{\nu_t}{\sigma_z}\right)\frac{\partial \zeta}{\partial x_j}\right] - \frac{\beta_5}{R_k + \delta}\,\zeta^{3/2}\\
&\quad + \left(\alpha_3 \zeta b_{ij} + \frac{1}{3}\delta_{ij}\zeta\right) S_{ij} - \frac{\zeta \tau_{ij}\Omega_i\Omega_j\beta_4}{\rho k \Omega}\\
&\quad + 2\varepsilon_{ilm}\beta_8\left(\frac{\tau_{ij}}{\rho k}\right)\left(\frac{\partial k}{\partial x_i}\frac{\partial \zeta}{\partial x_m}\right)\frac{\Omega_j}{S^2} - \frac{2\beta_6\tau_{ij}\nu_t}{\rho k \nu}\,\Omega\Omega_i\Omega_j\\
&\quad + \frac{\beta_7\zeta}{\Omega^2}\,\Omega_i\Omega_j S_{ij} + \max\left(\frac{DP}{Dt}, 0\right)\frac{k\Omega\rho}{\nu P \sigma_p}\end{aligned} \tag{5}$$

where

$$\begin{gathered}R_k = \frac{k}{\nu\sqrt{\zeta}}, \qquad \nu_t = \frac{\mu_t}{\rho}, \qquad S = \sqrt{S_{ij}S_{ij}}, \qquad \Omega = \sqrt{\Omega_i\Omega_i}\\
R_T = \frac{k^2}{\nu\zeta}, \qquad \zeta = \overline{\omega_i'\omega_j'}, \qquad \omega_i' = \varepsilon_{ilm}\partial_l u_m'\\
\Omega_i = \varepsilon_{ilm}\partial_l U_m, \qquad S_{ij} = \frac{1}{2}\left(\frac{\partial U_i}{\partial x_j} + \frac{\partial U_j}{\partial x_i}\right)\\
\tau_{ij} = \overline{-\rho u_i' u_j'} = \mu_t\left(2S_{ij} - \frac{2}{3}\delta_{ij}\frac{\partial U_m}{\partial x_m}\right) - \frac{2}{3}\rho k \delta_{ij}\end{gathered} \tag{6}$$

τ_k is a representative decay time for the kinetic energy, and ν_t is the kinematic eddy viscosity. The closure coefficients for the model are given in Table 1.

As may be seen from the governing equations, one needs to specify ν_t and τ_k for each mechanism to effect closure. For subsonic Mach numbers and regions where crossflow instability is unimportant, the dominant mode of instability is the first mode, or the T–S mode. Thus, when T–S waves are considered, ν_t is chosen as[5]

$$\nu_t = C_\mu k \tau_{\mu_l} \tag{7}$$

Table 1 k-ζ model constants

Constants	$k-\zeta$
C_μ	0.09
κ	0.40
α_3	0.35
β_4	0.42
β_5	2.37
β_6	0.10
β_7	1.50
β_8	2.30
σ_r	0.07
σ_p	0.065
$1/\sigma_k$	1.80
$1/\sigma_\zeta$	1.46
δ	0.1

where

$$\tau_{\mu_l} = \tau_{\mu_{l,TS}} = a/\omega \tag{8}$$

ω is the frequency of the first mode disturbance having the maximum amplification rate, and a is a model constant that depends on the freestream intensity, Tu, defined as

$$Tu = 100\sqrt{\tfrac{2}{3}(k_\infty/Q_\infty^2)} \tag{9}$$

In Eq. (9), Q_∞ is the freestream velocity. The frequency ω is given by a correlation developed by Walker[14] as

$$\omega\nu/Q_e^2 = 3.2 Re_{\delta^*}^{-3/2} \tag{10}$$

where Q_e is the velocity at the edge of the BL, and Re_{δ^*} is the edge Reynolds number based on a displacement thickness δ^*. The preceding correlation is based on the results of stability calculations for Falkner–Skan profiles obtained by Obremski et al.[15] and, thus, is suited for flows where the pressure gradient is not necessarily zero. The model constant a was correlated using flat-plate experiments by Schubauer and Klebanoff[16] and Schubauer and Skramstad[17] as (Ref. 5)

$$a = 0.069(Tu - 0.138)^2 + 0.00819 \tag{11}$$

Within the laminar region, the representative decay time for the kinetic energy is

$$1/\tau_{k_l} = a(\nu_t/\nu)S \tag{12}$$

The situation where transition is a result of CF instabilities is discussed next. The dominant mode of instability for the majority of swept-wing flows is the crossflow instability.[18,19] The BL on wings of moderate or high sweep generally contains significant crossflow. The velocity profile in this case can be separated into a component in the streamwise direction and a component in the crossflow direction. Because the crossflow profile always contains an inflection point, a strong inflectional instability is expected in regions when the crossflow velocity increases rapidly. This increase occurs in regions of negative pressure gradient, e.g., near the leading edge. In this favorable pressure gradient region, streamwise or T–S instabilities are stabilized and CF instability dominates the transition process.

As discussed in Refs. 18 and 19, the wavelength of the dominant crossflow disturbance varies with the BL thickness, δ. In addition to freestream disturbance levels, CF instabilities are sensitive to surface roughness. Using this information, an expression for the CF viscosity time scale was developed in Ref. 6 as

$$\tau_{\mu_l} = \tau_{\mu_{l,CF}} = (a + f)(\lambda_{CF}/Q_e) \tag{13}$$

where λ_{CF} is the wavelength of crossflow disturbances. Based on numerous experimental and computational results that found wavelengths of CF disturbances between three and four times the BL thickness, we use here

$$\lambda_{CF} = 3.5\delta \tag{14}$$

The use of Eq. (13) implies that a is representative of intensities that result in natural transition. Thus, the equation is not expected to hold for situations where $a \gg f$.

Because stationary CF disturbances are generated by surface roughness and traveling disturbances are generated by freestream disturbances and surface conditions, a correlation reflecting the influence of surface conditions must be included in the model. Using one of the sets reported by Radeztsky et al.,[20] f was correlated as[6]

$$f = 0.003[(h/h_{\text{ref}})^{-0.8}Re_h - 0.92] \tag{15}$$

where

$$h_{\text{ref}} = 1\ \mu\text{m} \tag{16}$$

$$Re_h = Q_\infty h/\nu_\infty \tag{17}$$

and h is the *peak-to-peak* distributed roughness level. The decay time for the kinetic energy is chosen as

$$1/\tau_{k_l} = (a + f)(\nu_t/\nu)S \tag{18}$$

Following the work of Robinson and Hassan,[13] the turbulent region time scales are given by

$$\tau_{k_t} = \tau_{\mu_t} = k/\nu\zeta \tag{19}$$

Because the thrust of this work is the prediction of transition onset, a simple intermittency approach is used in the transition region. As a result

$$\tau_\mu = (1 - \Gamma)\tau_{\mu_l} + \Gamma\tau_{\mu_t} \tag{20}$$

$$1/\tau_k = (1 - \Gamma)(1/\tau_{k_l}) + \Gamma(1/\tau_{k_t}) \tag{21}$$

The intermittency, Γ, is given by Dhawan and Narasimha's[1] expression, i.e.,

$$\Gamma(x) = 1 - \exp(-0.412\xi^2) \tag{22}$$

with

$$\xi = \max(x - x_t, 0)/\lambda \tag{23}$$

λ is a characteristic extent of the transitional region. An experimental correlation between λ and x_t is

$$Re_\lambda = 9.0Re_{x_t}^{0.75} \tag{24}$$

with x_t being the location where turbulent spots first appear, or where shin friction is minimum. It is shown in the work of Warren and Hassan[5] that this location is well represented by the relation

$$R_T = (1/C_\mu)(\nu_t/\nu) = 1.0 \tag{25}$$

Thus, x_t is the minimum location where $R_T \geq 1$.

Results and Discussion

Results presented here employed both boundary-layer and NS codes. The BL code is an adaptation of the code developed by Harris and Blanchard.[21] In addition to incorporating the present transition/turbulence model, it was extended to handle infinite swept wings. The NS code is an adaptation of an earlier code developed by Gaffney et al.,[22] which employs an upwind Roe scheme and four-step Runge–Kutta time-stepping method. When employing a BL code, the pressure distribution is obtained from an Euler code or experiment.

The BL code requires specifying starting conditions and these were chosen as the freestream conditions for both k and ζ and the other flow properties. The intensity in the tunnel and freestream velocity provide k_∞ from Eq. (9). Intensity measurements should be available for most facilities. On the other hand, ζ_∞ is determined from requiring $(\nu_t/\nu)_\infty \simeq 10^{-2}$ or some smaller number. It is found that results are not sensitive to the value of ζ_∞. Characteristic boundary conditions are used in the NS solver.

Transition resulting from T–S instabilities is discussed first. Figure 1 compares predictions of present theory with measurements over a flat plate.[16] With the current model, the only environmental condition that needs to be specified is the freestream turbulence level. Both computational schemes give similar results with regard to onset and extent of transition. The transition onset locations predicted by the present method are compared with the flat-plate experiments of Schubauer and Klebanoff[16] and Schubauer and Skramstad[17] in Table 2. As seen from the table, excellent results are obtained for all freestream intensities reported.

The rms amplitude ratio of the velocity disturbance can be obtained from the kinetic energy of the fluctuations as

$$A = \sqrt{k} = \sqrt{(\overline{u'^2} + \overline{v'^2} + \overline{w'^2})/2} \tag{26}$$

For the natural transition process there is a region of linear growth, followed by a region of nonlinear growth that occurs as the amplitude of the velocity disturbance becomes sufficiently large. Transition occurs after the onset of the nonlinear growth and this nonlinear growth continues through the transitional region. After the nonlinear growth region the modes that make up the disturbance become saturated. This saturation of modes characterizes the turbulent region. Figure 2 is a plot of the amplitude ratio as calculated by the present method for laminar flow, i.e., $\Gamma = 0$, with k_0 representing the initial amplitude of k. As can be seen from the figure, the present method does predict the expected linear, nonlinear, and saturated regions.

The next set of comparisons involve the data of Mateer et al.[23] They presented skin friction measurements over a supercritical airfoil for a freestream Mach number, M_∞, 0.2, and a range of Reynolds numbers and angles of attack, α. Moreover,

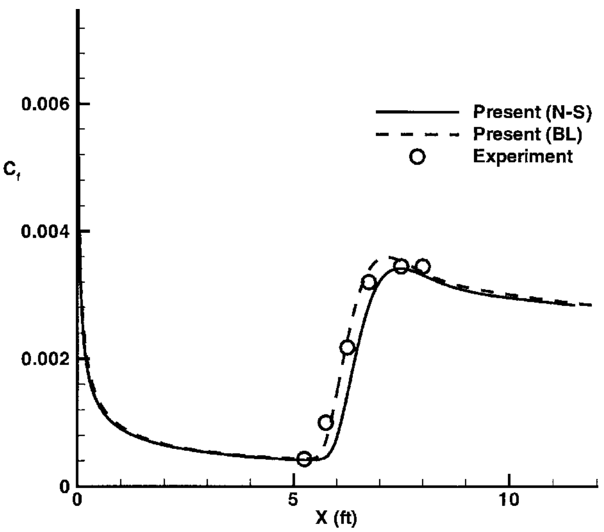

Fig. 1 Comparison of present method with the experiment of Schubauer and Klebanoff,[16] $Re = 1.67 \times 10^6$/m, NS and BL codes.

Table 2 Flat-plate experiments[a]

Case	Tu	X_t, ft Experiment	Current method	Error, %
Schubauer-Klebanoff[16]	0.03	5.26	5.39	2.47
Schubauer-Skramstad[17]	0.042	5.25	5.24	0.19
Schubauer-Skramstad[17]	0.10	5.08	4.86	4.3
Schubauer-Skramstad[17]	0.20	4.05	4.08	0.74
Schubauer-Skramstad[17]	0.26	3.32	3.41	2.7
Schubauer-Skramstad[17]	0.34	2.58	2.52	2.3

[a] $M_{ref} = 0.071$, $P_{ref} = 1.01325 \times 10^5$ Pa, T_{ref} 293 K.

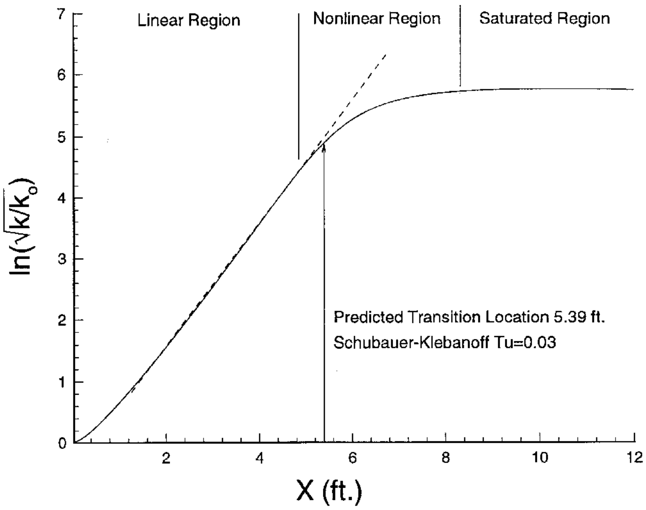

Fig. 2 Amplitude ratio vs distance along plate, Schubauer and Klebanoff experiment.[16]

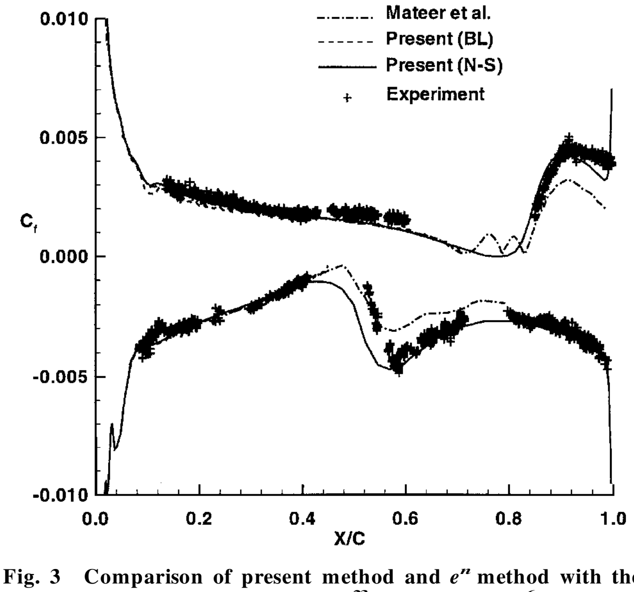

Fig. 3 Comparison of present method and e^n method with the airfoil experiment of Mateer et al.,[23] $Re_c = 0.6 \times 10^6$, $\alpha = -0.5$ deg.

because the e^n method requires a local stability analysis of the laminar BL, which is quite costly in addition to contributing to a lack of robustness, comparison was made with the transition method of Drela and Giles.[24] This method, which correlates the growth of the disturbances to the integral properties of the BL is an approximation to the e^n method with $n \sim 9$. Reference to the e^n method (in the following text), implies the procedure used in Ref. 23 to determine transition onset. Emphasis will be placed on comparisons with $a = -0.5$-deg cases because this is the angle of attack where large discrepancies between the e^n method and experimental data were noted. It

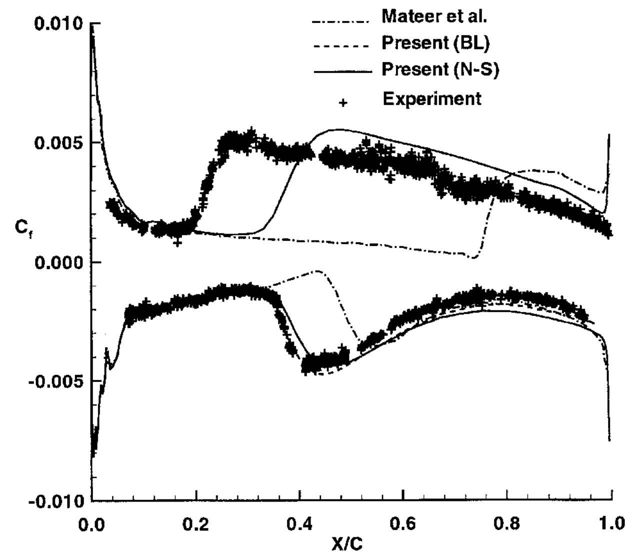

Fig. 4 Comparison of present method and e^n method with the airfoil experiment of Mateer et al.,[23] $Re_c = 2 \times 10^6$, $\alpha = -0.5$ deg.

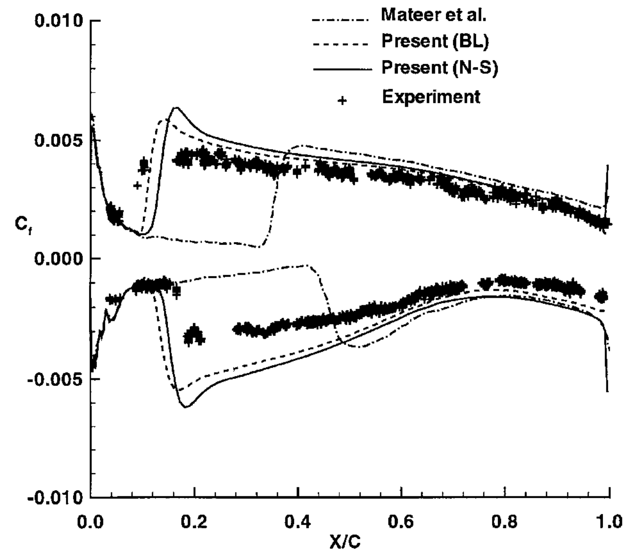

Fig. 5 Comparison of present method and e^n method with the airfoil experiment of Mateer et al.,[23] $Re_c = 6 \times 10^6$, $\alpha = -0.5$ deg.

is suggested that the e^n method is incapable of predicting transition for these cases when transition is dominated by Reynolds number effects and not determined solely by laminar separation.[23]

Figures 3–5 show a comparison of predictions of present theory with experiment and calculations reported in the work of Mateer et al. Both BL and NS calculations are shown. It is to be noted that when transition is a result of flow separation, BL calculations are terminated at separation. Figure 3 compares results for $Re_c = 2 \times 10^6$, Fig. 4 shows that the present method gives much better agreement than the e^n method with experiment for both upper and lower surfaces. A similar conclusion is reached for $Re_c = 6 \times 10^6$ as shown in Fig. 5. It is to be noted, however, that for this case, the current model overpredicts skin friction over part of the airfoil while giving reasonable estimates of onset location. It is difficult to pinpoint the cause of the discrepancy in skin friction for this case, particularly when good agreement for the other cases was indicated. Possible contributing factors may be the expression used to describe intermittency or increased blockage in the tunnel.

For higher angles of attack, the present and e^n methods are somewhat comparable in their predictions. Figure 6 compares calculations for $\alpha = 3.5$ deg and $Re_c = 2 \times 10^6$. It is to be noted that both models overestimate skin friction on the upper surface. For the upper surface, both models predict transition at the location of separation. However, for the lower surface, the present method predicts a location slightly upstream of the location of laminar separation. For this case, the e^n method predicts transition at the location of laminar separation for both upper and lower surfaces.

The next set of comparisons address transition resulting from crossflow instabilities. Figure 7 shows the coordinate system used for the swept-wing and swept-plate geometries. For these cases, available data give transition onset locations.[20,25–27] Unfortunately, skin friction data are not provided. Moreover, flow separation does not play any role in determining transition onset in available data. As a result, computations presented for CF instabilities were based on a three-dimensional BL code suited for calculating infinite swept wings. For such flows, the BL equations do not depend on the spanwise coordinate.[28]

The infinite swept wing experiments of Dagenhart et al.[25] and Radeztsky et al.[20] use a 45-deg swept wing with a NLF(2)-0415 cross section at −4-deg angle of attack. Figure 8 compares the experimental pressure coefficient on the upper surface of the NLF(2)-0415 airfoil with the computed results used in the present study. Transition onset was determined by naphthalene flow visualization. The experiments of Müller and Bippes[27] and Deyhle and Bippes[26] employed swept flat plates under the action of favorable pressure gradients. The pressure coefficient measured in the experiment is shown in Fig. 9 for the three tunnels used in the tests. Transition onset was determined by the location where $\Gamma = 0.5$.

To facilitate comparisons with experiment, transition onset was selected to be the point where $\Gamma = 0.5$. This assumes that the data reported in Radeztsky et al.[20] corresponds to a location where $\Gamma = 0.5$. As noted from Fig. 10, which compares present theory with the data of Radeztsky et al., excellent agreement is noted for all Reynolds numbers and surface finishes. For rms measured levels of surface roughness, a sinusoidal distribution is assumed and a peak-to-peak roughness level is established by multiplying the rms value by $\sqrt{2}$. The calculations assume a freestream intensity, $Tu = 0.09$, reported by Dagenhart.[29]

Table 3 compares present predictions with measurements reported by Deyhle and Bippes using three different facilities and a variety of surface finishes. The 1-MK tunnel is the 1×0.07 m^2 DLR facility in Göttingen, the NWB tunnel is the 3.25×2.8 m^2 DLR facility in Braunschweig, and the NWG tunnel

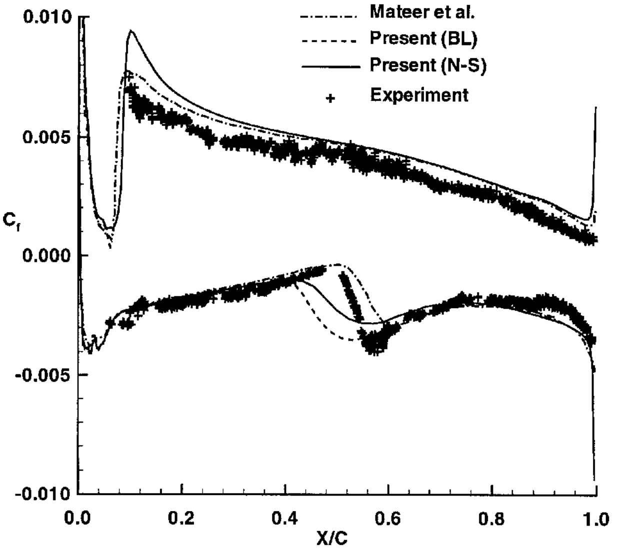

Fig. 6 Comparison of present method and e^n method with the airfoil experiment of Mateer et al.,[23] $Re_c = 2 \times 10^6$, $\alpha = 3.5$ deg.

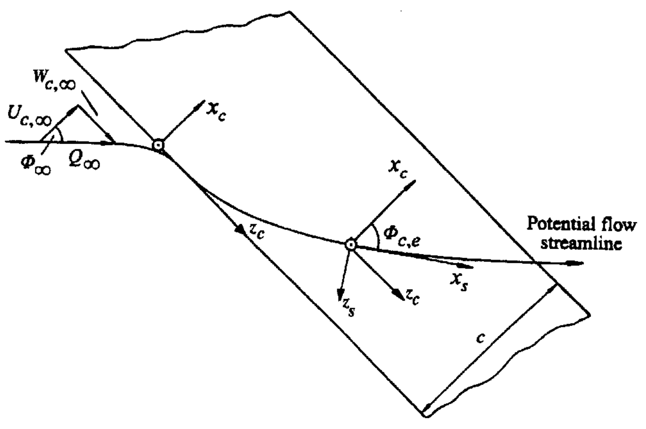

Fig. 7 Coordinate system on the swept wing and flat plate.

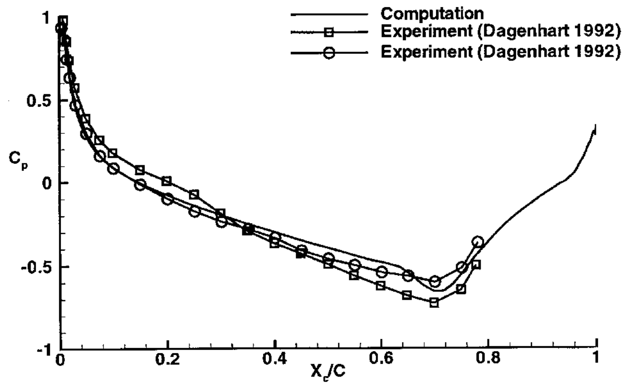

Fig. 8 Comparison of experimental and computed pressure coefficient on the upper surface of the NLF(2)-0415 airfoil.

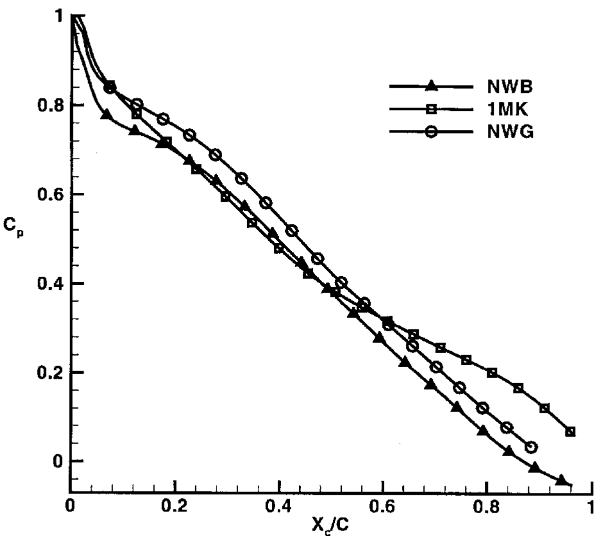

Fig. 9 Experimental pressure coefficient along the swept plate of Deyhle and Bippes.[26]

Table 3 Comparison of $Re_{x,tr}$ values at 50% intermittency[a]

Facility	Tu	Plate surface	$Re_{x,tr}$ ($\times 10^5$) Experimental	Present	Error (%)
NWB	0.08	Wooden plate, $\bar{R}_z = 6$ μm	6.5	8.04	23.7
1MK	0.15	Plate with sandpaper, $\bar{R}_z = 40$ μm	6.8	6.12	10.0
		Wooden plate, $\bar{R}_z = 6$ m	7.5	7.49	0.13
		Aluminum plate, sanded, $\bar{R}_z = 5$ μm	7.7	7.63	0.9
		Aluminum plate, polished, $\bar{R}_z = 1.8$ μm	8.3	8.48	2.17
1 MK/screen	0.27	Aluminum plate, polished, $\bar{R}_z = 1.8$ μm	7.8	7.11	8.85
NWG	0.57	Aluminum plate, sanded, $\bar{R}_z = 5$ μm	5.4	2.18	59.6

[a]Predicted by the present method and measured in the swept plate experiments of Deyhle and Bippes.[26]

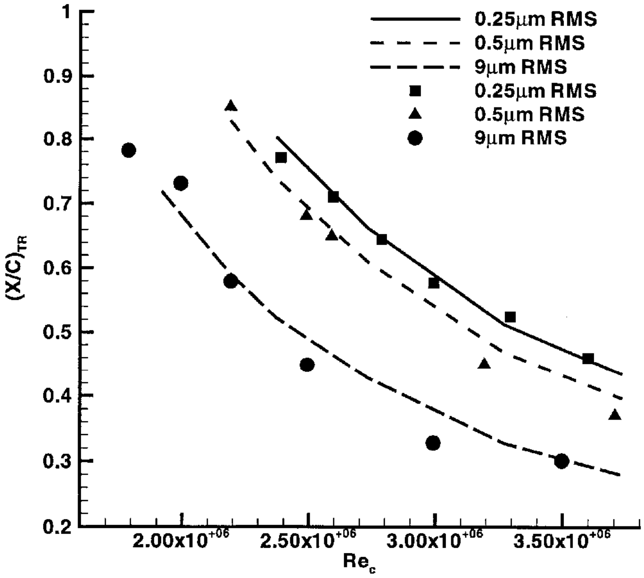

Fig. 10 Comparison of the present method with the experimental data of Radeztsky et al.[20]

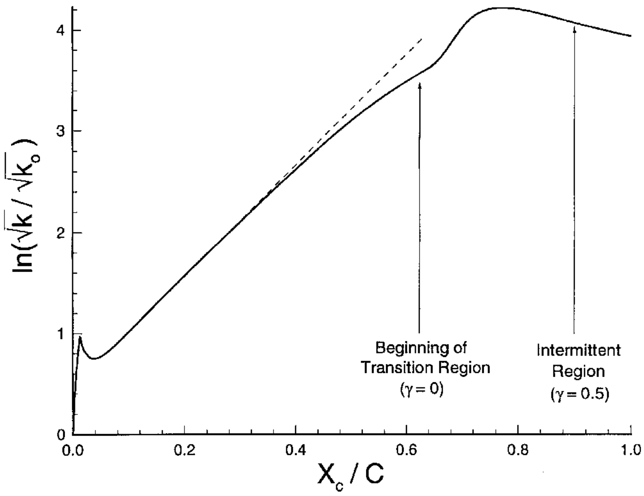

Fig. 11 Amplitude ratio vs distance, Deyhle and Bippes[26] swept plate, Tu = 0.15, $\bar{R}_z$ = 6 μm.

is the 3 × 3 m^2 DLR facility in Göttingen. As may be seen from the table, excellent agreement is indicated for measurements taken in the 1-MK facility. However, onset is overpredicted in the NWB tunnel and underpredicted in the NWG tunnel. The cause of the discrepancy in the NWB tunnel is not clear. On the other hand, the intensity in the NWG facility is high enough so that a bypass mechanism may have been present.

Figure 11 is a plot of the amplitude for the Tu = 0.15 and 6-μm roughness case in the 1-MK tunnel. Again, k_0 represents the kinetic energy of the fluctuations at the initial station, and is equal to k_∞. As seen from the figure, the present method predicts a region of linear growth and a significant region of nonlinear growth as the onset of transition is approached. The disturbance level tends to saturate as onset is approached but resumes exponential growth when transition region is entered. This agrees qualitatively with the large eddy simulation results presented by Huai and Joslin.[30]

Concluding Remarks

The present approach has developed, in the context of a CFD tool that employs turbulence modeling, a unified description for laminar, transitional, and turbulent flows. It allows for the presence of nonturbulent fluctuations and treats them in a manner similar to that of turbulent flows. As a result, one can calculate the complete flowfield without having to use stability codes and at a cost comparable to that of existing CFD codes that employ two-equation turbulence models.

Although the e^n method or linear stability codes were not used in the calculations, results of stability theory played an important role in determining expressions for the eddy viscosity resulting from laminar fluctuations. Because the physics underlying T–S or CF instabilities is different, corresponding stress–strain relations describing the flowfield are different. Further work is needed to develop a constitutive stress–strain relation that encompasses the effects of all relevant instabilities.

The preceding results represent the first step toward the practical application of a relatively simple closure model, which is based on the results of linear stability theory, for the prediction of the onset of transition. Because linear stability theory was developed using concepts of BL theory, frequencies having the maximum amplification rate were correlated in terms of δ, δ*, and edge velocity. Although calculation of such quantities is an inconvenience when employing two-dimensional NS solvers, they represent more of a challenge when employing three-dimensional NS solvers. Thus, future work should concentrate on developing correlations that depend on quantities other than δ, δ*, etc. Similar comments apply to the need for developing expressions for intermittency that are geometry independent.

Acknowledgments

This work is supported in part by NASA Grant NAG-1-1876. Part of the computations were carried out at the North Carolina Supercomputing Center and at the Numerical Aerospace Simulation (NAS) facilities. This paper was presented as SAE Paper 97-5502 at the 1997 World Aviation Congress, October 13–16, 1997, Anaheim, California. The authors are indebted to a number of colleagues for providing relevant data and publications and for many helpful discussions. They are Bill Saric of Arizona State University, Hans Bippes of DLR, German Aerospace Center, Ron Joslin and the late Ray Dagenhart of NASA Langley Research Center, and Nd Chokani from North Carolina State University.

References

[1]Dhawan, S., and Narasimha, R., "Some Properties of Boundary Layer Flow During Transition from Laminar to Turbulent Motion,"

Journal of Fluid Mechanics, Vol. 3, No. 4, 1958, pp. 418–436.
[2]Haynes, T. S., Reed, H. L., and Saric, W. S., "CFD Validation Issues in Transition Modeling," AIAA Paper 96-2057, June 1996.
[3]Young, T. W., Warren, E. S., Harris, J. E., and Hassan, H. A., "New Approach for the Calculation of Transitional Flows," *AIAA Journal*, Vol. 31, No. 4, April 1993, pp. 629–636.
[4]Warren, E. S., Harris, J. E., and Hassan, H. A., "A Transition Model for High-Speed Flow," *AIAA Journal*, Vol. 33, No. 8, 1995, pp. 1391–1397.
[5]Warren, E. S., and Hassan, H. A., "An Alternative to the e^n Method for Determining Set of Transition," AIAA Paper 97-0825, Jan. 1997.
[6]Warren, E. S., and Hassan, H. A., "A Transition Model for Swept Wing Flows," AIAA Paper 97-2245, June 1997.
[7]Robinson, D. F., Harris, J. E., and Hassan, H. A., "Unified Turbulence Closure Model for Axisymmetric and Planar Free Shear Flows," *AIAA Journal*, Vol. 33, No. 12, 1995, pp. 2325–2331.
[8]Wilcox, D. C., "Turbulence Model Transition Prediction," *AIAA Journal*, Vol. 13, No. 2, 1975, pp. 241–243.
[9]Wilcox, D. C., "Alternative to the e^9 Procedure for Predicting Boundary-Layer Transition," *AIAA Journal*, Vol. 19, No. 1, 1991, pp. 56–64.
[10]Wilcox, D. C., "The Remarkable Ability of Turbulence Model Equations to Describe Transition," 5th Symposium on Numerical and Physical Aspects of Aerodynamic Flows, California State Univ., Long Beach, CA, Jan. 1989.
[11]Chang, C.-L., Singer, B. A., Dinavahi, S. P. G., El-Hady, N. M., Harris, J. E., Street, C. L., and Wilcox, D. C., "Transition Region Modeling for Compressible Flow," National Aerospace Plane, CR 1142, Feb. 1993.
[12]Wilcox, D. C., "Turbulence and Transition Modeling for High-Speed Flows," NASA CR 19147, April 1993.
[13]Robinson, D. F., and Hassan, H. A., "Modeling Turbulence Without Damping Functions Using k-ζ Model," AIAA Paper 97-2312, June 1997.
[14]Walker, G. J., "Transitional Flow on Axial Turbomachine Blading," *AIAA Journal*, Vol. 27, No. 5, 1989, pp. 595–602.
[15]Obremski, H. J., Morkovin, M. V., and Landahl, M., "Portfolio of Stability Characteristics of Incompressible Boundary Layer," AGARDograph 134, March 1969.
[16]Schubauer, G. B., and Klebanoff, P. S., "Contributions on the Mechanics of Boundary-Layer Transition," NACA Rept. 1289, March 1956.
[17]Schubauer, G. B., and Skramstad, H. K., "Laminar Boundary Layer Oscillations and Transition on a Flat Plate," NACA Rept. 909, 1948.
[18]Saric, W. S., "Physical Description of Boundary Layer Transition: Experimental Evidence," AGARD Rept. 793, March 1993.
[19]Arnal, D., "Boundary Layer Transition Prediction, Application to Drag Reduction," AGARD Rept. 786, March 1992.
[20]Radeztsky, R. H., Jr., Reibert, M. S., Saric, W. S., and Takagi, S., "Effect of Micron-Sized Roughness on Transition in Swept-Wing Flows," AIAA Paper 93-0076, Jan. 1993.
[21]Harris, J. E., and Blanchard, D. K., "Computer Program for Solving Laminar, Transitional, or Turbulent Compressible Boundary-Layer Equations for Two-Dimensional and Axisymmetric Flow," NASA TM 83207, Feb. 1982.
[22]Gaffney, R. L., Jr., Salas, M. D., and Hassan, H. A., "An Abbreviated Reynolds Stress Turbulence Model for Airfoil Flows," AIAA Paper 90-1468, June 1990.
[23]Mateer, G. G., Monson, D. J., and Menter, F. R., "Skin-Friction Measurements and Calculations on a Lifting Airfoil," *AIAA Journal*, Vol. 34, No. 2, 1996, pp. 231–236.
[24]Drela, M., and Giles, B. G., "Viscous-Inviscid Analysis of Transonic and Low Reynolds Number Airfoils," *AIAA Journal*, Vol. 25, No. 10, 1987, pp. 1347–1355.
[25]Dagenhart, J. R., Saric, W. S., Hoos, J. A., and Mousseux, M. C., "Experiments on Swept Wing Boundary Layers," *Laminar-Turbulent Transition IUTAM Symposium* (Toulouse, France), edited by D. Arnal and R. Michel, Springer–Verlag, Berlin, 1989.
[26]Deyhle, H., and Bippes, H., "Disturbance Growth in an Unstable Three-Dimensional Boundary Layer and Its Dependence on Environmental Conditions," *Journal of Fluid Mechanics*, Vol. 316, June 1996, pp. 73–113.
[27]Müller, B., and Bippes, H., "Experimental Study of Instability Modes in a Three-Dimensional Boundary Layer," AGARD Rept. 438, Oct. 1988.
[28]Schlichting, H., *Boundary-Layer Theory*, 7th ed., McGraw–Hill, New York, 1979.
[29]Dagenhart, J., "Crossflow Stability and Transition Experiments in a Swept-Wing Flow," Ph.D. Dissertation, Virginia Polytechnic Inst. and State Univ., Blacksburg, VA, 1992.
[30]Huai, X., and Joslin, R. D., "Large-Eddy Simulation of Laminar-Turbulent Transition in a Swept-Wing Boundary-Layer," AIAA Paper 97-0750, Jan. 1997.